MAGNETIC FIELD CHARACTER OF TPS BOOSTER MAGNETS*

J.C. Jan[#], C.Y. Kuo, C.H. Chang, Y.L. Chu, Y.T. Yu, F.Y. Lin, H.H. Chen, H.M. Huang, C.S. Yang, C.S. Hwang, NSRRC, 101 Hsin-Ann Road, Hsinchu Science Park, Hsinchu 30076, Taiwan

Abstract

Taiwan Photon Source (TPS) will be a 3-GeV synchrotron radiation facility operated with top-up injection. The booster ring of TPS shares the same tunnel concentric with the storage ring. The lattice of the booster is a 24-cell DBA of circumference 496.8 m. The energy of the electron beam is ramped from 150 MeV to 3 GeV at repetition rate 3 Hz in the booster ring. The trajectory of the electron beam is controlled by complicated magnets that include combined dipole magnet, combined quadrupole magnet, pure quadrupole magnet, sextupole magnet and corrector magnet. The measurement, analysis and performance of the combined dipole and combined quadrupole magnets are discussed in this letter.

INTRODUCTION

The booster ring of TPS is composed of 54 combined dipole magnets, 36 pure quadrupole magnets (BR-QP), 48 combined quadrupole magnets (BR-QF) and 24 sextupole magnets (BR-SM) [1-3]. The field parameters of these magnets are listed in Table 1. The combined dipole magnets have two types with magnetic field lengths 1.6 m (BR-BD) and 0.8 m (BR-BH).

Table 1: Parameters of the TPS Booster Ring Magnet

	BD	BH	QP	QF	SM
b_0L (Tm)	1.3104	0.6552	-	-	-
b_1L (T)	-2.7575	-1.3787	4.2985 -2.7174 -1.2623	3.3780	-
b_2L (Tm^{-1})	-9.8714	-4.9357	-	3.8678	-
b_1L/b_0L (m^{-1})	-2.1043	-2.1043	-	-	-
b_2L/b_0L (m^{-2})	-7.5331	-7.5331	-	-	-
b_2L/b_1L (m^{-1})	-	-	-	1.1450	-
L_{eff} (m)	1.6	0.8	0.3	0.3	0.2

*b_2 denotes sextupole entire coefficient, b_2 = k2/2!

COMBINED DIPOLE MAGNET

The first prototype of the BR-BD-P01a magnet was finished in year 2011. The main field of the dipole magnet is distorted by the lift hole and the lamina winding of the yoke. The second prototype of the BR-BD-P01b magnet was improved on increasing the thickness of the yoke to avoid saturation of the magnetic flux and decreasing the field distortion. The yoke thickness of BR-BD-P01b was increased 30 mm in the vertical direction and 20 mm in the horizontal direction. The third prototype of the BR-BD-P01c magnet improved the content of the quadrupole and sextupole components to meet more closely the TPS requirement. The slope of the pole tip was increased and an end chamfer of the magnet was cancelled to optimize the quadrupole and sextupole components in the combined dipole magnet.

The general magnetic field of the magnet can be expressed with equation (1) on the axis, (Y=0). Hence, X, Y and Z are the transverse direction, vertical direction and direction marks the trajectory of the electron beam, respectively. The B_yL, b_0L, b_1L, b_2L and b_3L are the integral general field, integral dipole component, integral quadrupole component, integral sextupole component and integral octupole component, respectively. The method using polynomial fitting to obtain multipoles is called a fitting method; see equation (1). Moreover, another method to obtain multipoles use differential equation is called a differential method; see equations (2) and (3).

$$B_yL = b_0L + b_1L \times X + b_2L \times X^2 + b_3L \times X^3 + ... \quad (1)$$

$$\frac{\partial B_yL}{\partial X} = b_1L + 2 \times b_2L \times X + 3 \times b_3L \times X^2 + ... \quad (2)$$

$$\frac{\partial^2 B_yL}{\partial X^2} = 2 \times b_2L + 6 \times b_3L \times X + ... \quad (3)$$

Figures 1 (a) and (b) display the central homogeneity ($\Delta b_0/b_0$) and integral homogeneity ($\Delta b_0L/b_0L$) of BR-BH-001, BR-BD-002 and a TOSCA simulation at current 987 A. $\Delta b_0/b_0$ and $\Delta b_0L/b_0L$ are calculated after subtracting the quadrupole and sextupole components. $\Delta b_0/b_0$ and $\Delta b_0L/b_0L$ of BR-BH-001 (BR-BD-002) are better than 4.5×10^{-4} (-3.0×10^{-4}) and 1.9×10^{-4} (-5.3×10^{-4}) in the good field region, respectively.

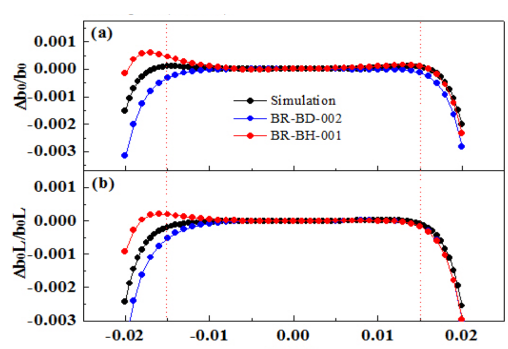

Figure 1: Homogenity of the centeral field and integral field of BR-BH-001 and BR-BD-002 magnet, comparison with simulation at 987 A.

*This work was supported in part by the National Science Council of Taiwan under Contract No. NSC 99-2221-E-213-003-MY3
[#] janjc@nsrrc.org.tw

The normalized integral field of general field (B_yL/I) and calculated value of the BR-BH-001 magnet with varied excitation current is displayed in Fig. 2 (a). The black solid-triangle and open-triangle symbol lines are B_yL with current excited upward and downward, respectively. The discrepancy between B_yL/I and b_0L/I is 0.027 % along the current excited downward, not shown here. The main contribution of B_yL/I is b_0L/I and other multipole contributions is hence tiny. The red solid-triangle symbol line is the calculated value of b_0L/I of BR-BH-001 according to equation (4) with yoke relative permeability μ_r and remnant field B_r ignored. Here, μ_0 denotes the permeability of vacuum, N the number of coils, g the pole gap, L the flux loop in the yoke and L_{eff} the effective length. The measurement of B_yL/I is confirmed by the calculated value with μ_r and B_r ignored between 100 A and 900 A. That B_yL/I of the BR-BH-001 magnet is clearly increasing is due to the remnant field effect at low current. That B_yL/I of the BR-BH-001 magnet is slowly decreasing is due to the yoke situation over 900 A. Figures 2 (b) and (c) display the b_1L/I and b_2L/I of the BR-BH-001 magnet analyzed by the fitting and differential methods. b_1L/I obtained agree from both methods. Moreover, b_2L/I have random fluctuations analyzed by the fitting method; b_1L/I and b_2L/I of the BR-BD-002 magnet have the same behavior as the BR-BH-001 magnet, not shown here. The measured quadrupole (b_1L/b_0L) and sextupole (b_2L/b_0L) ratio with varied excitation current are displayed in Fig. 3 (a) and (b), respectively. The measured b_1L/b_0L and b_2L/b_0L with the differential method analysis are -2.1085 m^{-1} and -6.7449 m^{-2} at 987 A, respectively.

$$\frac{b_0L}{I} = \left(\frac{\mu_0 N}{g + \frac{L}{\mu_r}} + B_r\right) \times L_{eff} \qquad (4)$$

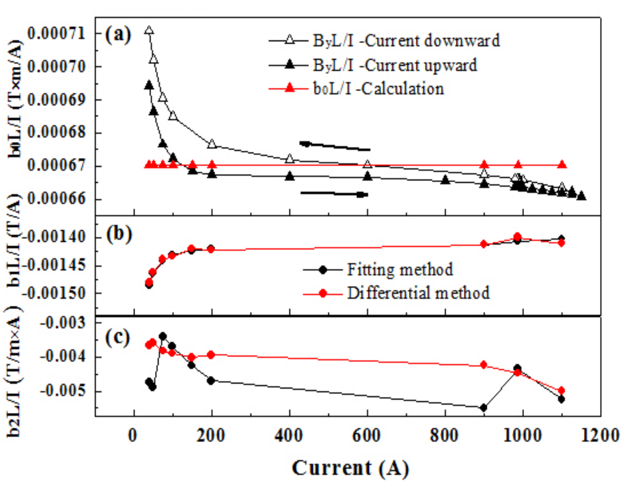

Figure 2: (a) B_yL/I of the BR-BH-001 magnet with current excited along downward, upward and calculation. (b) b_1L/I analyzed by the fitting and differential methods. (c) b_2L/I analyzed by the fitting and differential methods.

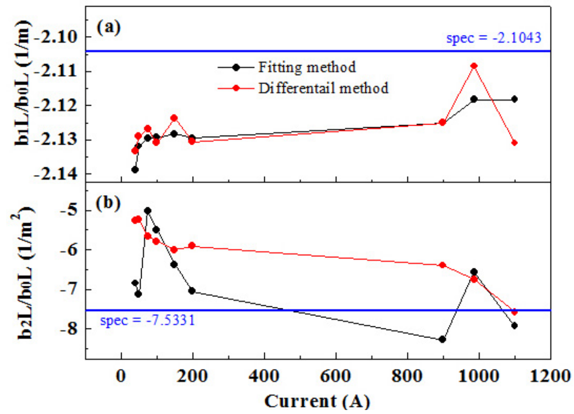

Figure 3: (a) and (b) display ratios b_1L/b_0L and b_2L/b_0L with the differential method analysis of the BR-BH-001 magnet at 987 A.

Figure 4 displays the simulation and measured multipole distribution with varied excitation current along the trajectory of the electron beam. The excitation currents 50 A, 987 A and 1100 A correspond to electron energies 150 MeV, 3 GeV and 3.3 GeV, respectively. The simulation of the multipole distribution used the TOSCA 3D module and is displayed with the open-circle line in Fig. 4. The measured multipole distributions agree with the simulation result at 987 A.

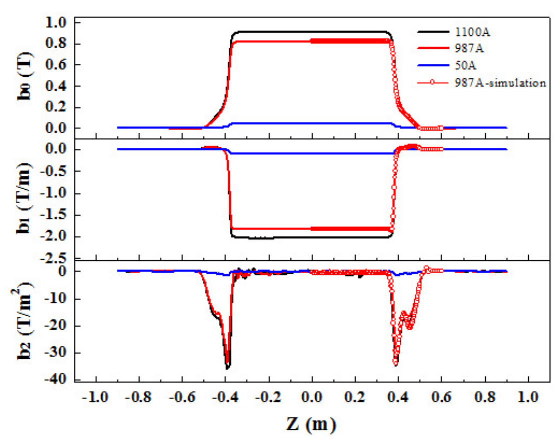

Figure 4: The multipole distributions at 50, 987, 1100 A and the simulation along trajectory of the electron beam.

COMBINED QUADRUPOLE MAGNETS

The booster ring of TPS has 48 combined quadrupole (BR-QF) magnets. The field qualities of these BR-QF magnets are examined with the rotating-coil measurement system (RCS) at the vendor and vendee sites [4]. The measured and normalized radii of RCS are 16 mm and 15 mm, respectively. Figures 5 (a) and (b) display the integral quadrupole field strength (b_1L) and integral sextupole field strength (b_2L) of 19 BR-QF magnets with varied current at the vendor site, respectively. The mean value and standard deviation of b_1L are 3.3647 T (0.2280 T) and 0.0032 T (0.0004 T) at 82 A (5 A), respectively. The mean value and standard deviation of b_2L are 3.7871

ISBN 978-3-95450-122-9

T/m (0.2602 T/m) and 0.0356 T/m (0.0161 T/m) at 82 A (5 A), respectively. Ratio b_1L/b_2L of BR-QF is displayed in Fig. 5 (c). The mean value and standard deviation of b_2L/b_1L are 1.1256 m^{-1} (1.1409 m^{-1}) and 0.0101 m^{-1} (0.0695 m^{-1}) at 82 A (5 A), respectively. The b_2L/b_1L dispersion at 5 A is larger than at 82 A, because the remnant field obviously influences at the low current. The dispersion of the sextuple component will be compensated by the booster sextupole magnet.

The normalized normal-term (B_nL/B_1L) and skew-term (A_nL/B_1L) of the BR-QF magnets with currents excited 82 A and 5 A are display in Fig. 6 and 7. The circle black-symbol line and triangle red-symbol line are for currents excited 82 A and 5 A, respectively. B_5L/B_1L and B_8L/B_1L are the first allowed terms of the quadrupole and sextupole multipoles, respectively. B_3L/B_1L and B_4L/B_1L are forbidden terms of the magnet. All multipole distributions, except B_3L/B_1L and B_5L/B_1L, are quite similar at 82 A and 5 A. The different B_3L/B_1L is caused by the remnant field between 82 A and 5 A. The different B_5L/B_1L is from the yoke edge between 82 A and 5 A. This behavior is demonstrated by the Hall probe measurement, not shown here.

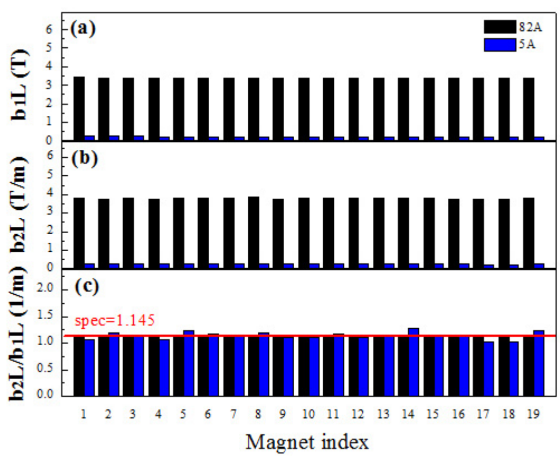

Figure 5: (a) and (b) display b_1L and b_2L at currents excited 5 A and 82 A. (c) displays the multipole ratio b_2L/b_1L at currents excited 5 A and 82 A.

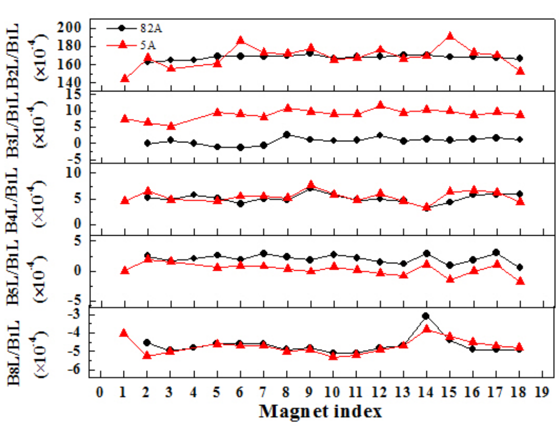

Figure 6: Normalized normal-multipole of BR-QF magnets at 82 A and 5 A.

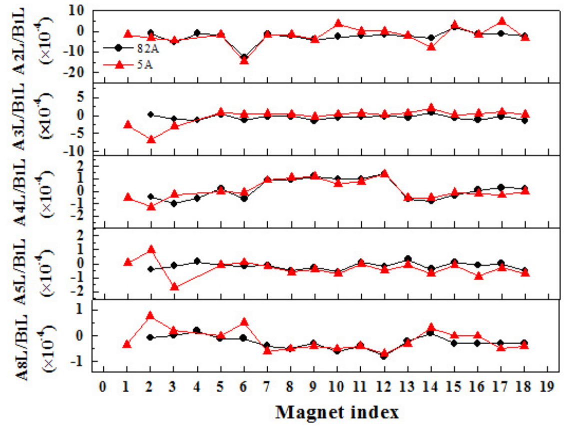

Figure 7: Normalized skew-multipole of BR-QF magnets at 82 A and 5 A.

SUMMARY

Construction of the combined dipole magnet is beginning after the third prototype improvement. The field homogeneities $\Delta b_0/b_0$ and $\Delta b_0L/b_0L$ of the BR-BH-001 (BR-BD-002) prototype are close to the simulation after subtracting the combined components, respectively. The normalized dipole field strength b_0L/I is agree with calculation value between 100 A and 900 A. The effects of remnant field and field situation of the magnet has an impact below 100 A and over 900 A, respectively. The differential method was used to analyze the quadrupole and sextupole components in the combined dipole magnet. The multipole distribution of the combined dipole magnet was demonstrated with simulation along the Z-axis. The b_2L/b_1L dispersion of the BR-QF magnet with current excited 5 A is larger than at 82 A, because the remnant field obviously has an influence at a low current. The dispersion of the sextuple component will be compensated by the booster sextupole magnet. Moreover, the remnant field causes the B_3L/B_1L to differ between excitation currents 82 A and 5 A. The booster magnets are under construction and will be finished at 2013 September.

REFERENCES

[1] C.S. Hwang *et. al.,* " Status of magnet design for the accelerator lattice of the TPS projrct", Proceedings of PAC 09, Vancouver, BC, Canada. pp. 196-198 (2009).

[2] C.Y. Kuo *et. al.,* "Development of combined function magnets for the Taiwan photon source", Proceedings of PAC 09, Vancouver, BC, Canada. pp.202-204 (2009).

[3] J.C. Huang *et. al.,* "The effect of eddy currents on the homogeneity of the magnetic field of a booster-ring sextupole magnet", Proceedings of PAC 09, Vancouver, BC, Canada. pp.193-195 (2009).

[4] J.C. Jan *et. al.,* "Crosstalk issues of vicinity magnets studied with a novel rotating-coil system", MT22, 4KP2-1 (2011).